Available online at www.sciencedirect.com
ScienceDirect
Tetrahedron
Tetrahedron 63 (2007) 232–240

Synthesis of oligo(*p*-phenylene vinylene)-porphyrin-oligo(*p*-phenylene vinylene) triads as antenna molecules for energy transfer

Tonggang Jiu,[a,b] Yongjun Li,[a,b] Haiyang Gan,[a,b] Yuliang Li,[a,b,*] Huibiao Liu,[a,b] Shu Wang,[a,b] Weidong Zhou,[a,b] Chunru Wang,[a,b] Xiaofang Li,[a,b] Xiaofeng Liu[a,b] and Daoben Zhu[a,b,*]

[a]*Beijing National Laboratory for Molecular Sciences (BNLMS), CAS Key Laboratory of Organic Solids, Institute of Chemistry, Chinese Academy of Sciences, Beijing 100080, PR China*
[b]*Graduate School of Chinese Academy of Sciences, Chinese Academy of Sciences, Beijing 100080, PR China*

Received 17 May 2006; revised 8 October 2006; accepted 10 October 2006
Available online 30 October 2006

Abstract—The oligo(*p*-phenylene vinylene)-porphyrin-oligo(*p*-phenylene vinylene) (P-OPV*n*, *n*=2, 4, where *n* is the number of phenyl rings) and the complex with Zn^{2+} based on P-OPV*n* were synthesized for investigating their photophysical properties via UV–vis, voltammetry, steady-state and time-resolved fluorescence spectra. In these molecules two OPV moieties as energy donors were linked to porphyrin center by virtue of Wittig reaction. The detailed studies of photophysical properties indicate that OPV group can act as an antenna unit for effective intramolecular energy transfer.

1. Introduction

Studies of supramolecular systems bearing redox and photoelectronic entities are valuable for designing light energy harvesting systems as well as for developing redox and optoelectronic devices[1,2]. Covalent linkage of donor–acceptor entities with one or more spacer units to control the distance and orientation has been the popular choice[2] even though noncovalent linkage is considered to be nature's choice of assembling the different redox and photoactive entities in the active centers of biological systems.[3] To fully exploit the benefits of these interesting materials, there is a need for supramolecular systems with antenna unit. Antenna molecules, as interesting optoelectronic devices, have attracted much attention in which one chromophore at one end of the array can absorb photon and the other chromophore at the opposite end of the array will emit photon subsequently. For this purpose, a few elegantly designed donor–acceptor type diads and triads have been synthesized and studied.[2] OPV derivatives have been extensively studied on light-emitting materials, field-effect transistors, supramolecular assembly, and amphiphilic materials[4] due to their high absorption coefficient, strong donating ability, and good thermal, chemical, and photochemical stability.[5] Incorporating porphyrin within molecular donor–acceptor systems, in which porphyrin acts as an electron acceptor or donor linked with appropriate donor or acceptor, is a viable route to design photovoltaic and molecular electronics.[5] To the best of our knowledge, there are limited examples of connected systems prepared from porphyrin and oligo(*p*-phenylene vinylene)s,[5j,5k] revealing their unique photophysical and photochemical properties.

Here we would like to report the synthesis and characterization of a series of conjugated molecules in which OPV units are linked to porphyrin with different lengths and describe an ultrafast spectroscopic investigation of photoinduced energy migration dynamics that takes place on these efficient light-harvesting antenna supramolecules.

2. Results and discussion

2.1. Synthesis

The synthesis of a homologous series of oligo(*p*-phenylene vinylene)-porphyrin-oligo(*p*-phenylene vinylene) (P-OPV*n*, *n*=2, 4, where *n* is the number of phenyl rings) and oligo(*p*-phenylene vinylene)-porphyrin-Zn-oligo(*p*-phenylene vinylene) (P-OPV*n*-Zn, *n*=2, 4), are outlined in Scheme 1. The Wittig reaction, which generally gives a mixture of

Keywords: Energy transfer; Oligo(*p*-phenylene vinylene); Antenna; Fluorescence lifetime.
* Corresponding authors. Tel.: +86 10 62588934; fax: +86 10 82616576 (Y.L.); e-mail: ylli@iccas.ac.cn

0040–4020/$ - see front matter © 2006 Published by Elsevier Ltd.
doi:10.1016/j.tet.2006.10.029

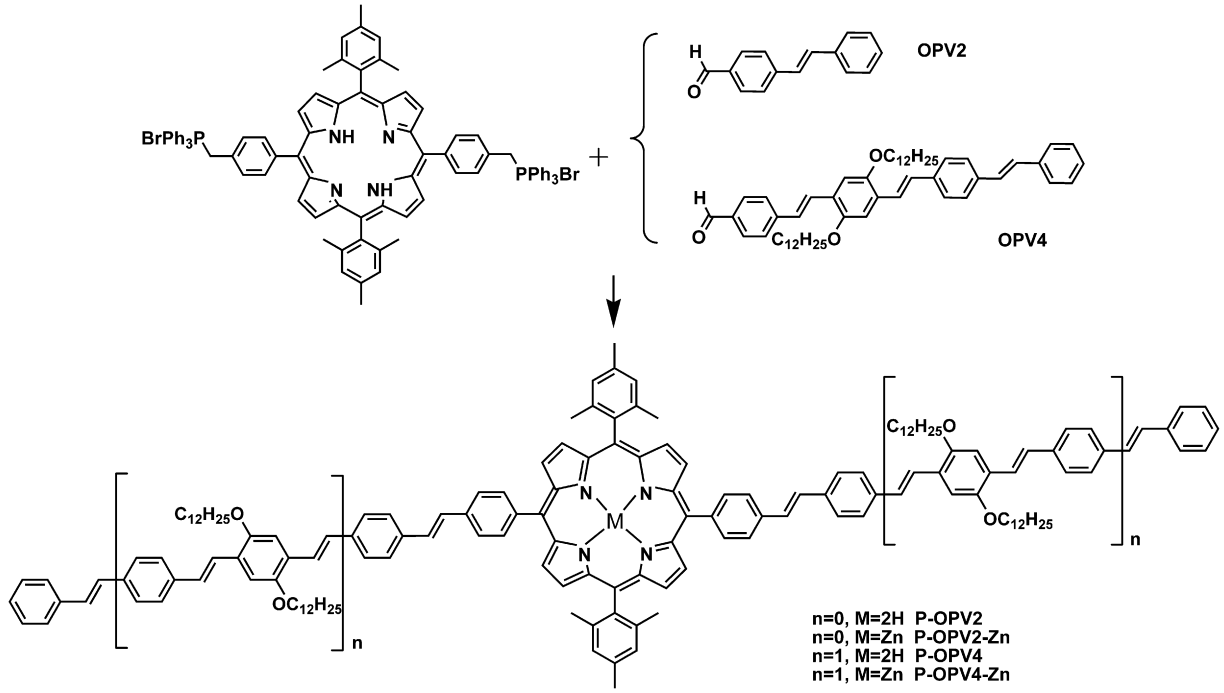

Scheme 1. Synthesis of P-OPV*n* and P-OPV*n*-Zn, *n*=2, 4.

cis- and trans-isomers, has been widely used to synthesize conjugated, conducting oligomers and polymers. By further exploration of this methodology, the keys for the preparation of the antenna molecules are for synthesizing the linear, different lengths phenylene vinylene oligomers and conjugated connecting with porphyrin-OPV moieties.

Several strategies have been developed to synthesize homologue series of laterally substituted OPV*n* in the past few years.[6] The general synthetic routes for OPV*n* are shown in Scheme 2. In order to facilitate Wittig reaction of a free-base porphyrin within two conjugated oligomer chains, 4-(bromomethyl)benzaldehyde reacted with *meso*-(mesityl)dipyrromethane with catalytic amounts of trifluoroacetic acid to yield the methyl halide substituted free-base porphyrin in 25% yield.[7] Large quantity of dipyrromethane can be readily prepared according to Lindsey et al.[8] P-OPV*n* (*n*=2 and 4) was prepared through a double Wittig reaction of porphyrin bisphosphonium salts and the corresponding OPV2 and OPV4 were obtained in low yields due to the formation of several isomers. Quantitative metalation of P-OPV*n* with $Zn(OAc)_2$ afforded P-OPV*n*-Zn. The structures of new compounds were characterized by ^{1}H NMR, MALDI-TOF mass spectroscopy, and elemental analysis. Their mp's were all greater than 300 °C. ^{1}H NMR spectra showed expected signals for the inner proton of free-base porphyrin chromophores at around −2.59 ppm together with the aromatic protons (at about 8.80 ppm) corresponding to pyrrole of porphyrin.

Because of rigidity and planarity of the π-conjugated phenylene vinylene units, unsubstituted PPV and higher homologues of related OPV*n* are highly insoluble. To preserve their unique characteristics (or functional properties) and alleviate their solubility problem, we have previously synthesized a series of highly light-emitting coplanar OPV3 containing three phenyl rings bearing solubilizing dialkoxy substituents such as hexyl, octyl, decyl, and dodecyl every second phenylene ring. By capping more solubilizing substituents at the side chain, highly soluble OPV*n* containing up to nine phenyl rings have been synthesized. To increase the solubility of P-OPV*n* and P-OPV*n*-Zn, long alkoxyl substituents were attached to the oligophenylene vinylene, a common strategy in soluble polymer preparation. The mesityl substituents on the porphyrin ring also contribute to the solubility.[9] Due to the presence of the substituents, the triads were soluble in common organic solvents such as toluene, CH_2Cl_2, $CHCl_3$, and THF. It also significantly reduced the π–π aggregation of the P-OPV*n* and the self-quench of porphyrin fluorescence.

2.2. Electrochemistry

The electrochemical data for the triads from cyclic voltammetry with Bu_4NPF_6 (0.04 M in *o*-dichlorobenzene) as supporting electrolyte in anodic oxidation and cathodic reduction are shown in Table 1. The voltammetries of P-OPV*n* (*n*=2, 4) and P-OPV*n*-Zn (*n*=2, 4) were carried out using 10^{-5} mol L^{-1} concentration. The occurrence of a cathodic redox process depended on the presence of OPV segment that can decrease the LUMO energy level of porphyrin. Both compounds present a partially reversible oxidation process around 1.08 V versus Ag wire. The CV analysis of P-OPV2 showed three reversible peaks in the redox part at −1.44, −1.78, and −1.98 V versus Ag wire. On the other hand, the potentials of oxidation wave were at 1.08 V and 1.40 V. The CV wave of P-OPV4 was similar to that of P-OPV2. It exhibited four reversible peaks in reduction wave and three irreversible peaks in oxidation wave. Almost similar electrochemical behaviors were observed for P-OPV*n*-Zn (Table 1). P-OPV2-Zn showed a partially reversible oxidation process and the oxide potentials were

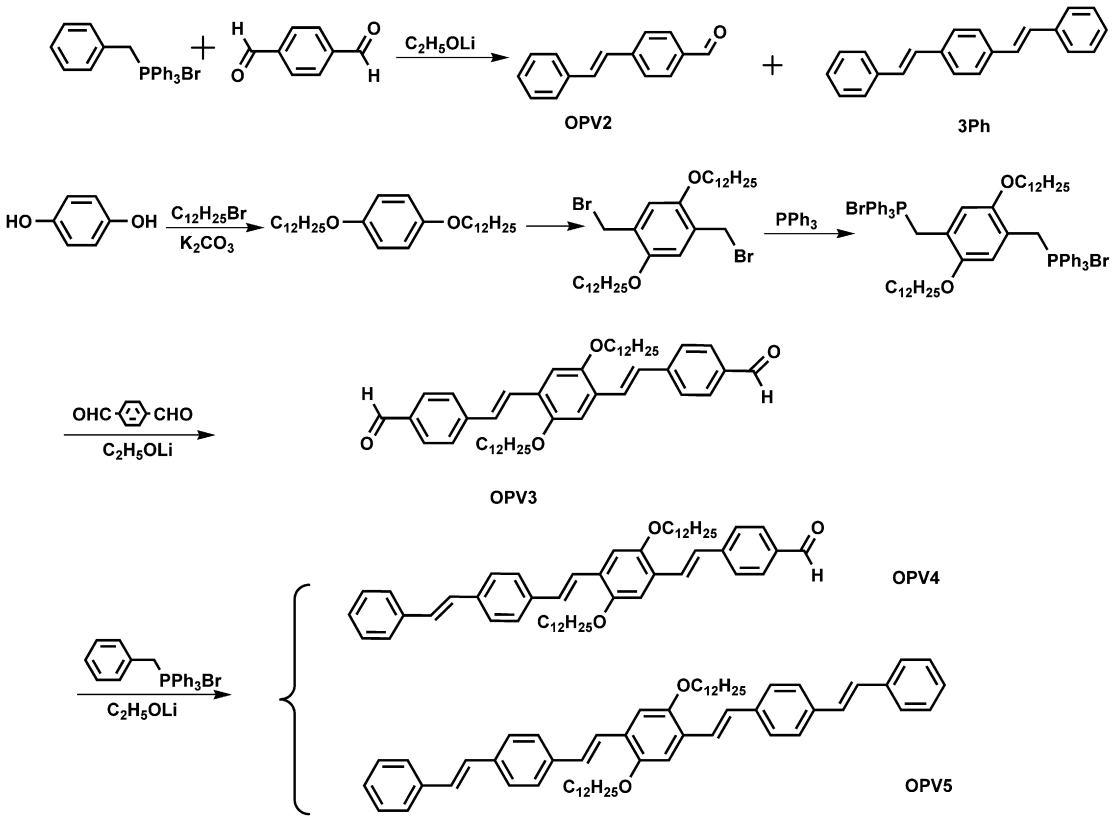

Scheme 2. Oligo(*p*-phenylene vinylene) monomer.

Table 1. Electrochemical data for the triads

Compound	Potential[a]/V						
	E_{ox}^{P3}	E_{ox}^{P2}	E_{ox}^{P1}	E_{red}^{P1}	E_{red}^{P2}	E_{red}^{P3}	E_{red}^{P4}
P-OPV2		1.40	1.08	−1.44	−1.78	−1.98	
P-OPV4	1.77	1.06	0.96	−1.02	−1.40	−1.74	−2.04
P-OPV2-Zn	1.49	1.12	0.56	−1.14	−1.71		
P-OPV4-Zn	1.73	1.18	0.87	−1.13	−1.44	−1.74	−2.05

[a] Cyclic voltammograms (CV) were performed in a solution of *o*-dichlorobenzene using Glassy carbon electrode as working electrode, platinum wire as counter electrode, and Ag electrode as the reference electrode at a scan rate of 20 mV/s at room temperature under the protection of nitrogen.

0.56, 1.12, and 1.49 V versus Ag wire. A comparison between the redox potentials of the P-OPV4 and that of the P-OPV4-Zn recorded under similar solution conditions revealed small shifts of 10–120 mV, suggesting the existence of ground-state interactions between the porphyrin π-ring and OPV moiety.

2.3. Steady-state absorption spectra

As shown in Figure 1, the absorption maxima of the P-OPV2 and P-OPV4 Soret bands (422 nm and 424 nm, respectively) were all slightly red-shifted and broader than that of the corresponding tetraphenylporphyrin (TPP) (418 nm) due to π-conjugation effect.[10] This phenomenon can be attributed to the presence of an intramolecular donor–acceptor framework between the porphyrin unit, an electron-withdrawing group, and OPV moiety, an electron-rich unit, which decreases the π–π* energy gap. There was no significant difference from 550 nm to 750 nm between P-OPV2 and P-OPV4, in the UV–vis spectra as an extended function of

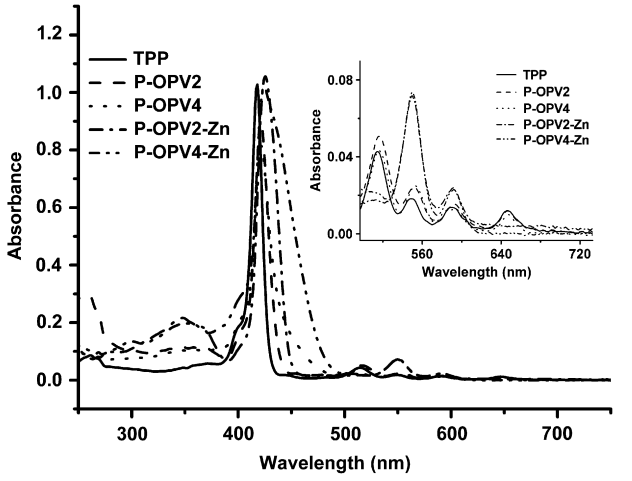

Figure 1. UV–vis absorption spectra recorded in chloroform solutions of P-OPV*n* (*n*=2, 4) and P-OPV*n*-Zn (*n*=2, 4) with concentration 2×10^{-6} mol/L. The inset is the corresponding Q bands absorption of P-OPV*n* and P-OPV*n*-Zn.

the conjugated length of the OPV units. The absorption spectra of P-OPV*n*-Zn showed the typical pattern of regular metal porphyrin with two Q bands in addition to the Soret band. Compared with that of TPP, the absorption bands of the P-OPV2-Zn (426 nm) and P-OPV4-Zn (425 nm) were obviously red-shifted and broader. This indicated that the π-conjugation of the Zn-porphyrin moiety was extended into the OPV spacer, allowing electronic communication between the two conjoint units in the ground and excited states. Also, the interaction between porphyrin ring and Zn contributed to the red shift of absorption spectra.

2.4. Emission measurements

Fluorescence spectra (422 nm excitation) of P-OPV*n* and P-OPV*n*-Zn in $CHCl_3$ solution are shown in Figure 2. The emission spectra of the OPV2, OPV4, and TPP are also shown for comparison. Both of P-OPV*n* (n=2, 4) exhibited an intense red emission peak at 651 nm with a shoulder around 716 nm when excited at 422 nm, while tetraphenylporphyrin (TPP)[11] showed two relatively weak emission peaks at around 650 nm and 714 nm. Upon incorporation of OPV*n* moiety into triads, compared with TPP the peaks (651 nm) of P-OPV*n* were broadened and slightly red-shifted. Energy transfer from OPV segments to porphyrin core led to this relatively red shift of porphyrin emission peak and the decrease of emission intensity of OPV. For P-OPV4, the remaining emission of the shoulder (467–493 nm) from OPV accounted for the competition between the direct emission from OPV unit and energy transfer to porphyrin. The fluorescence quantum yields (Φ_f) of P-OPV2 and P-OPV4 were found to be 13% and 14%, respectively. The fact that the fluorescence quantum yields of P-OPV*n* increase compared with TPP (Φ_f=0.11)[12] suggested that OPV group conjugated connecting with porphyrin core can promote the intramolecular energy transfer and increase the probability to generate the excited state due to increasing the absorption. The emission properties of P-OPV*n*-Zn and P-OPV*n* showed both similarity to and difference from one another. One similarity among all triads is that the emission occurred essentially from the porphyrin emission band even though the excitation light was absorbed primarily by the OPV component. This observation indicated efficient energy transfer from the excited oligo(*p*-phenylene vinylene) (OPV*) to the ground state of porphyrin and porphyrin-Zn. The difference is that P-OPV*n*-Zn showed a red emission peak at 600 nm with a shoulder around 650 nm when excited at 424 nm. The fluorescence photographs of P-OPV*n* (n=2, 4) and P-OPV*n*-Zn are inserted in Figure 2, along with the photographs of OPV*n* (n=2, 4) and TPP. As shown in Figure 2, when excited at 365 nm corresponding to the fluorescence spectra, P-OPV2 underwent a dramatic color change from blue of OPV2 to red, and P-OPV4 exhibited the intermediate color of red porphyrin and green OPV4. P-OPV*n*-Zn (n=2, 4) also showed interesting color change of nacarat and bottle green, respectively.

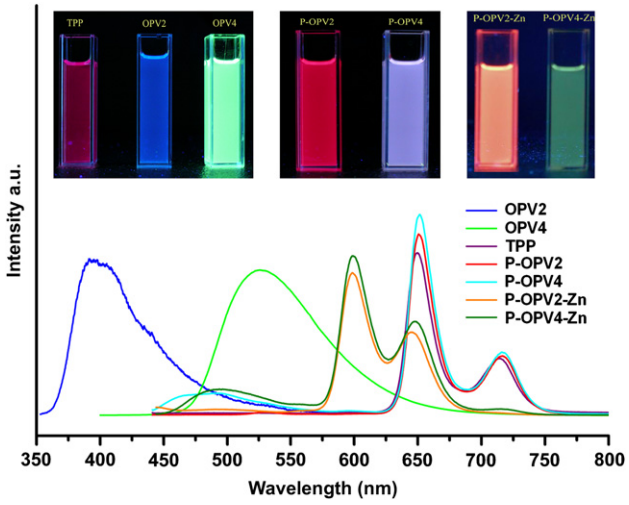

Figure 2. Normalized emission spectra recorded in chloroform solutions of P-OPV*n* (n=2, 4), P-OPV*n*-Zn, and TPP recorded at 5 nm slits with 422 nm excitation and OPV*n* with 333 nm, 380 nm excitations, respectively. *Inset*: fluorescence photographs of P-OPV*n*, P-OPV*n*-Zn, OPV*n*, and TPP recorded in chloroform solutions with 365 nm excited.

2.5. Steady-state fluorescence spectra comparison

The energy transfer behaviors of the triads have been studied by both steady-state and time-resolved fluorescence spectra. The changes of the fluorescence emission spectra of P-OPV*n* (n=2, 4) by changing the excitation wavelength with uniform concentration in $CHCl_3$ solution are shown in Figure 3. 3Ph and OPV5 were used as reference molecules to investigate the interaction between OPV moiety and porphyrin core in the triads. The emissions of P-OPV*n* were monitored using excitation at several wavelengths where either the OPV*n* or the porphyrin primarily absorbs. As shown in Figure 3a, upon irradiation of the triad at 351 nm, where the 3Ph absorption outclassed that of the porphyrin, the emission spectrum was dominated by porphyrin core fluorescence. Only a small amount of OPV moiety's excited-state fluorescence was observed. In Figure 3b, the spectra of P-OPV4 are similar to that of P-OPV2. The fluorescence of OPV5 segment attached to porphyrin remarkably decreased relative to OPV5 molecule excited at 421 nm. Comparison of the $S_1 \rightarrow S_0$ emission spectra of the various P-OPV*n*-Zn and OPV*n* revealed trends similar to those described above. Due to concentration quench effect the fluorescence properties were investigated at the concentration of 2×10^{-6} mol/L. The P-OPV2-Zn emission intensity in the region 375–550 nm was reduced significantly and red-shifted. The remains indicated that the P-OPV2-Zn in the excited state not only transfers energy to the middle Zn-porphyrin core but also returns to the ground state by emission at 450–490 nm. P-OPV4-Zn showed similar optical character by monitoring the emission band (450–500 nm). All these results showed that, when OPV*n* was attached to porphyrin (or Zn-porphyrin), the fluorescence of the OPV*n* moieties was significantly quenched as compared with OPV reference molecules and the fluorescence of the porphyrin core increased. This fully demonstrated the antenna effect of OPV moieties arranged on both sides of the central energy acceptor. For the reasons of the observed decrease of OPV*n* emission intensity, the occurrence of the following processes was suggested: excited energy transfer from OPV*n* to the porphyrin (or Zn-porphyrin) entity within the triads. This process is illustrated in Figure 4. In the following sections the time-resolved emission spectral results are discussed in order to verify the quenching pathways.

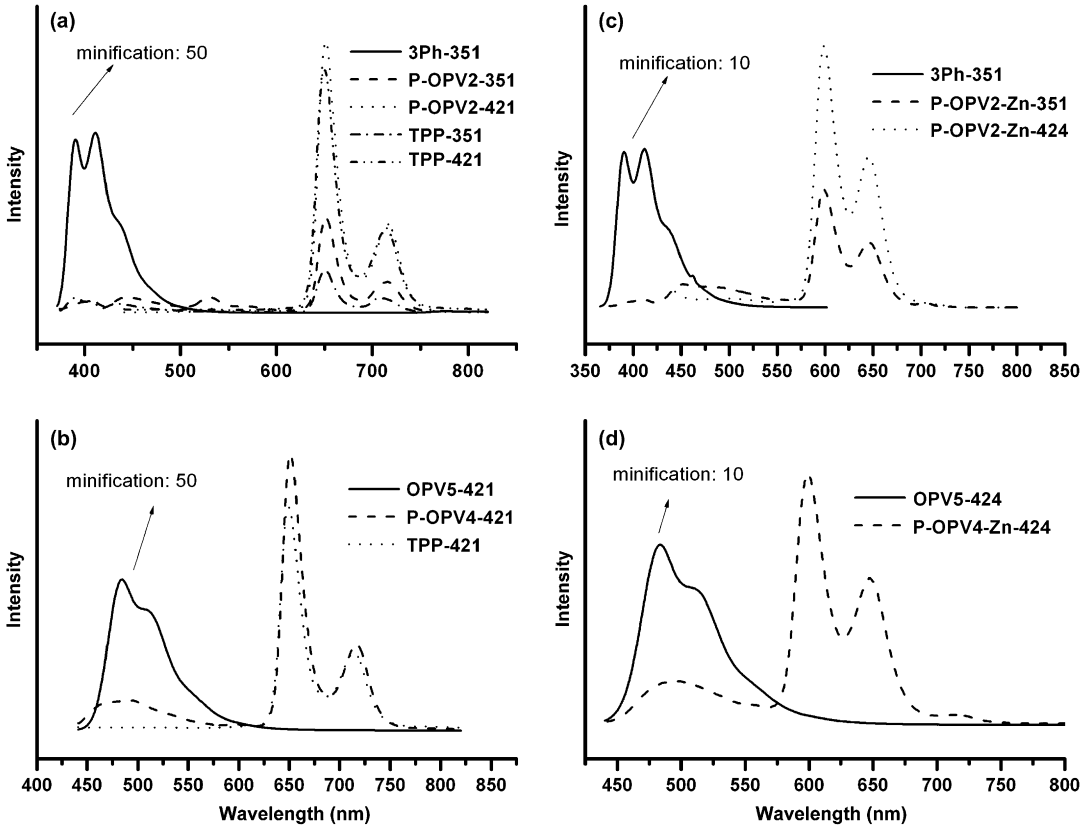

Figure 3. (a), (b) Steady-state fluorescence spectra of P-OPV*n* (*n*=2, 4), TPP, 3Ph, and OPV5 excited by different wavelengths recorded in chloroform solutions with uniform concentration (2×10^{-5} mol/L). (c), (d) Steady-state fluorescence spectra of P-OPV*n*-Zn (*n*=2, 4), 3Ph, and OPV5 recorded in chloroform solutions with uniform concentration (2×10^{-6} mol/L).

2.6. Time-resolved nanosecond fluorescence measurements

The dynamics of energy transfer behavior between the two chromophore units was examined by employing the time-resolved nanosecond fluorescence spectroscopy. The photophysical data are summarized in Table 2. Our experiment was performed in chloroform solution at room temperature. The experiments on lifetime measurements were carried out by exciting these triads at 400 nm and monitoring the OPV

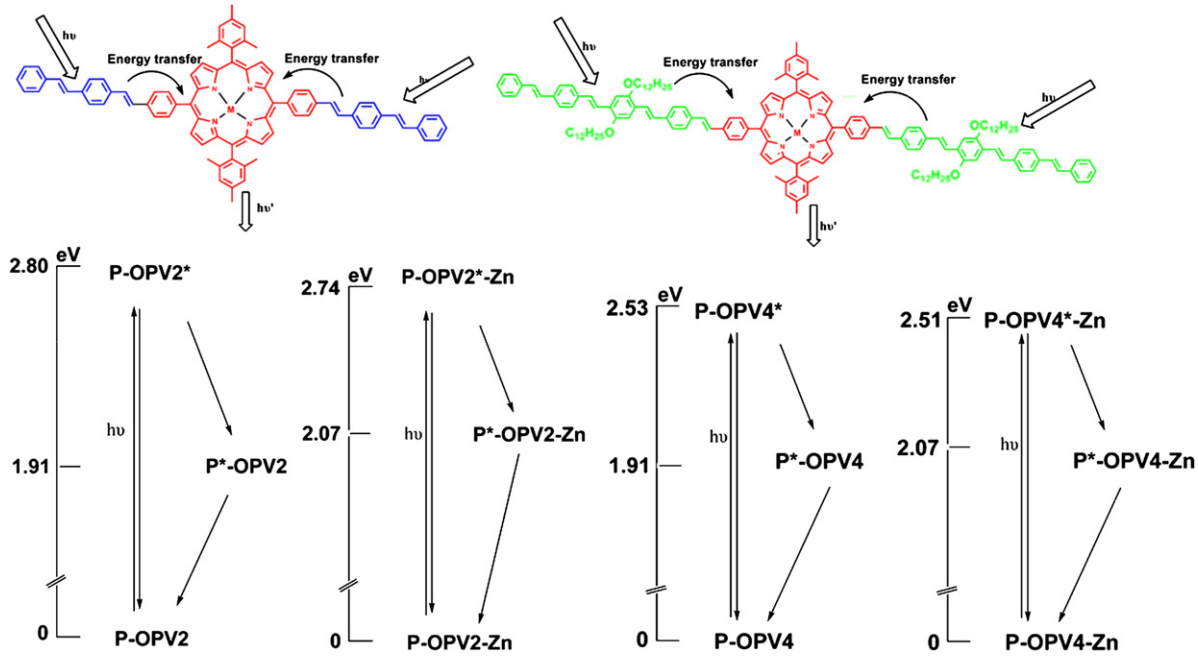

Figure 4. Energy level diagrams for the photoinduced energy transfer processes for the P-OPV*n* and P-OPV*n*-Zn triads. The excited-state energies were obtained from the absorption and emission spectra.

Table 2. Photophysical parameters of the triads (298 K) investigated in chloroform solution (0.1 mM)

Triads and monomer	Monitoring band	τ_1 (ns)	τ_2 (ns)	τ_{av} (ns)	Φ_f	k_{Ent} (s^{-1})
P-OPV2	OPV	0.167 (61%)	0.944 (39%)	0.47	0.13	3.3×10^{11}
	Porphyrin	1.02 (13%)	9.19 (87%)	8.12		
P-OPV4	OPV	0.254 (15%)	1.34 (85%)	1.17	0.14	2.1×10^{11}
	Porphyrin	1.08 (16%)	9.10 (84%)	7.81		
P-OPV2-Zn	OPV	1.54 (89%)	4.10 (11%)	1.82	0.027	2.6×10^{10}
	Porphyrin	2.00 (97%)	7.90 (3%)	2.18		
P-OPV4-Zn	OPV	1.13 (88%)	3.30 (12%)	1.39	0.056	4.0×10^{10}
	Porphyrin	1.90 (93%)	5.13 (7%)	2.13		
3Ph	OPV	1.16			0.99	
OPV5	OPV	1.14 (91%)	3.77 (9%)	1.38	0.9[14]	
Zn-TPP	Porphyrin			2.0[15]	0.030[12]	

moiety's emission band, where the emission spectrum was dominated by OPV fluorescence. The OPV*n* fluorescence time profiles of the triads, P-OPV2 and P-OPV4, could be fitted satisfactorily to biexponential decay. The short lifetimes of the components were found to be about 0.167 ns (61%) and 0.944 ns (39%) for P-OPV2, suggesting the occurrence of intramolecular energy transfer from the excited OPV2 to porphyrin in the triad. For P-OPV4 triads, the lifetime was found to be around 0.254 ns (15%) and 1.342 ns (85%), respectively. Similarly the porphyrin fluorescence time profiles of the triads were fitted satisfactorily to biexponential decay by monitoring the porphyrin-emission band at 651 nm. In addition, the excited-state lifetimes of P-OPV*n*-Zn (n=2, 4) were determined and the values are given in Table 2 along with those obtained previously for the comparative monomer. In general, the lifetimes for the Zn-porphyrin monomers were in the range 1.5–2.5 ns. By monitoring the Zn-porphyrin-emission band at 600 nm, the lifetimes of P-OPV*n*-Zn (2.18, 2.13 ns) were found to be longer than that of Zn-TPP (2.0 ns). Significantly, the porphyrin excited-state lifetimes of P-OPV*n* (n=2, 4) were 8.12 and 7.81 ns, respectively, which were shorter than that of the free-base porphyrin (13 ns), due to strong donor–acceptor interaction between OPV units and porphyrin. Compared with P-OPV*n*, the lifetimes of P-OPV*n*-Zn (n=2, 4) exhibited obvious decrease to 2.18 and 2.13 ns, respectively, these results indicated that a strong interaction existed between OPV unit and porphyrin (Zn) moiety.

$$k_{Ent} = \frac{(\Phi_{ref}/\Phi) - 1}{\tau_{ref}} \quad (1)$$

From Eq. 1,[13] combined with the steady-state data, it was possible to estimate the rate constant of the OPV → porphyrin energy transfer process, which turned out to be 3.3×10^{11} s^{-1} for P-OPV2 and 2.6×10^{10} s^{-1} for P-OPV2-Zn. In Eq. 1, Φ and Φ_{ref} are the OPV fluorescence quantum yields of the multicomponent triads and of the reference compounds, whereas τ_{ref} is the singlet lifetime of the latter. In the same way, the energy transfer rate constant for P-OPV4 and P-OPV4-Zn can be calculated as 2.1×10^{11} s^{-1} and 4.0×10^{10} s^{-1}, respectively. Altogether with the steady-state studies, this unique interaction may mainly attribute to the OPV antenna role as the result of energy transfer from OPV*n* to porphyrin (Zn) core; also, the electron transfer cannot be ruled out. We have obtained the average time constant (τ_{av}) out of these two decay components for the four triads shown in Table 2. This fluorescence quenching behavior of OPV moiety can be explained in terms of the enhanced energy transfer between the two moieties and the reduced intermolecular quenching, which resulted in an increase of the emission intensity of the porphyrin core.

3. Conclusions

In summary, we prepared a series of porphyrin-containing OPV antenna units based on a concise synthetic approach involving few building blocks. These molecules were functionalized with OPV groups as antenna unit for showing pure red emission. The energy transfer behavior between the two chromophore moieties was investigated by employing steady-state and time-resolved fluorescence spectra. Interestingly, compared with the lifetime values (8.12 and 7.81 ns, respectively) of P-OPV*n*(n=2, 4), the lifetimes of P-OPV*n*-Zn (n=2, 4) showed obvious decrease to 2.18 and 2.13 ns, respectively, These results indicated that the OPV antenna unit played a key role for the unique properties of energy transfer in the molecule system.

4. Experimental

4.1. Materials and instruments

Most of the chemical reagents were purchased from Acros or Aldrich Corp. and were utilized as received unless indicated otherwise. All solvents were purified using standard procedures. Column chromatography was performed on silica gel (size 160–200 mesh). UV–vis spectra were taken on a Hitachi U-3010 spectrometer, and fluorescence spectra were measured on a Hitachi F-4500 spectrofluorometer. Cyclic voltammograms (CV) were recorded on CHI660B voltammetric analyzer (CH Instruments, USA). The CV was performed in a solution of Bu_4NPF_6 (0.04 M) in *o*-dichlorobenzene at a scan rate of 20 mV/s at room temperature under the protection of nitrogen. Glassy carbon electrode was used as the working electrode and Pt wire was used as the counter electrode. An Ag electrode was used as the reference electrode. Time-resolved fluorescence spectra were measured using a photo-counting streak camera (C2909, amamatstu). This machine uses a femto-second laser source running at 1 KHz. The laser's output wavelength can be set to the desired excitation with OPA (OPA-800CF, Spectra Physics). The fluorescence lifetimes were measured on an Edinburgh Instruments Ltd FLS920. NMR spectra were obtained on a Bruker Avance DPS-400 (400 MHz)

spectrometer. MALDI-TOF mass spectrometric measurements were performed on a Bruker Biflex MALDI-TOF mass spectrometer.

4.1.1. 4-Styrylbenzaldehyde OPV2 and 1,4-distyrylbenzene 3Ph. To a solution of benzyltriphenylphosphonium bromide[16] (0.22 g, 0.5 mmol) and terephthalaldehyde (0.08 g, 0.6 mmol) in methylene chloride (25 mL) was added lithium ethoxide solution (1.5 mL, 1.0 M in ethanol) dropwise via a syringe at room temperature. The solution was stirred for 30 min. The solvent was then removed from the resulting solution under reduced pressure. A solution of this isomer mixture and iodine (20 mg) in methylene chloride (50 mL) was stirred at room temperature overnight. The dark brown solution was then diluted with methylene chloride and washed consecutively with aqueous $Na_2S_2O_3$ solution (1.0 M, 2×25 mL) and water. After concentration on a rotary evaporator, this solution was loaded onto a silica gel column and eluted with a mixture of hexane and methylene chloride (1:1 v/v). This afforded 0.07 g of OPV2 and 3Ph as fluorescent solids. The solids were dissolved in methylene chloride and purified by flash chromatography. ^{1}H NMR ($CDCl_3$) δ (ppm) OPV2: 7.07 (d, 1H, J=16.0 Hz), 7.19 (d, 1H, J=17.5 Hz), 7.28 (d, 1H, J=7.0 Hz), 7.35 (t, 2H, J=7.6 Hz), 7.49 (d, 2H, J=8.0 Hz), 7.57 (d, 2H, J=8.0 Hz), 7.80 (d, 2H, J=8.0 Hz), 9.93 (s, 1H). MS (EI): 208 (M).

3Ph: 7.12 (s, 4H), 7.24–7.28 (m, 2H), 7.36 (t, 4H, J=7.2 Hz), 7.51 (s, 6H), 7.53 (s, 2H). MS (EI): 282 (M).

4.1.2. 2,5-Bis(dodecyloxy)-1,4-bis(4-formylphenylene vinylene) benzene. OPV3. A suspension of 1,4-bis(bromomethyl)-2,5-bis(dodecyloxy)benzene[16] (1 g, 1.59 mmol) and triphenylphosphine (0.87 g, 3.32 mmol) in toluene was heated at reflux for 10 h. The solvent was then removed from the resulting solution under reduced pressure. The resulting residue, along with terephthalaldehyde (0.425 g, 3.17 mmol), was dissolved in methylene chloride (50 mL). To this solution was added lithium ethoxide solution (4 mL, 1.0 M in ethanol) dropwise via a syringe at room temperature. The base should be introduced at such a rate that the transient red-purple color produced upon the addition of base should not persist. The resulting solution was allowed to stir for further 10 min after the completion of base addition. Then this reaction was quenched by aqueous HCl. The organic layer was separated, washed with water, and dried over anhydrous sodium sulfate. The residues, after removal of solvents, contained both *E*- and *Z*-isomers. A solution of this isomer mixture and iodine (500 mg) in methylene chloride (50 mL) was stirred at room temperature overnight. The dark brown solution was then diluted with methylene chloride and washed consecutively with aqueous $Na_2S_2O_3$ solution (1.0 M, 2×75 mL) and water. After concentration on a rotary evaporator, this solution was loaded onto a silica gel column and eluted with methylene chloride. This afforded 0.78 g of OPV3 as a yellow fluorescent solid. Yield 70%. ^{1}H NMR ($CDCl_3$): δ (ppm) 0.87 (t, 6H, J=8.0 Hz), 1.10–1.41 (m, 36H), 1.85–1.92 (m, 4H), 4.08 (t, 4H, J=8.4 Hz), 7.15 (s, 2H), 7.18 (s, 1H), 7.23 (s, 1H), 7.60 (s, 2H), 7.67 (d, 4H, J=8.4 Hz), 7.87 (d, 4H, J=9.2 Hz), 10.00 (s, 2H). MALDI-TOF MS: *m*/*z*: 706 $[M+H]^+$.

4.1.3. 4-(4-(4-Styrylstyryl)-2,5-bis(dodecyloxy)styryl)-benzaldehyde OPV4 and 1,4-bis(4-styrylstyryl)-2,5-bis-(dodecyloxy)benzene OPV5. To a solution of benzyltriphenylphosphonium bromide (0.86 g, 1.99 mmol) and OPV3 (1.40 g, 1.99 mmol) in methylene chloride (50 mL) was added lithium ethoxide solution (2.5 mL, 1.0 M in ethanol) dropwise via a syringe at room temperature. The solution was stirred for 20 min. The solvent was then removed from the resulting solution under reduced pressure. The mixture and iodine (500 mg) in methylene chloride (50 mL) was stirred at room temperature overnight. The dark brown solution was then diluted with methylene chloride and washed consecutively with aqueous $Na_2S_2O_3$ solution (1.0 M, 2×75 mL) and water. After concentration on a rotary evaporator, this solution was loaded onto a silica gel column and eluted with a mixture of petroleum ether and methylene chloride (1:1 v/v). This afforded 0.62 g of OPV4 and 0.34 g of OPV5 as fluorescent solids. ^{1}H NMR ($CDCl_3$): δ (ppm) OPV4: 0.87 (d, 6H, J=3.6 Hz), 1.25–1.55 (m, 36H), 1.87–1.89 (m, 4H), 4.04–4.09 (m, 4H), 7.12–7.16 (m, 5H), 7.18–7.20 (m, 2H), 7.37 (t, 2H, J=7.2 Hz), 7.48–7.52 (m, 7H), 7.61–7.67 (m, 3H), 7.87 (d, 2H, J=7.6 Hz), 9.99 (s, 1H). MALDI-TOF MS: *m*/*z*: 780 $[M+H]^+$.

OPV5: 0.87 (s, 6H), 1.15–1.36 (m, 36H), 1.88–1.89 (m, 4H), 4.03–4.08 (m, 4H), 7.12–7.13 (m, 6H), 7.23–7.25 (m, 6H), 7.34–7.39 (m, 4H), 7.52 (s, 8H). MALDI-TOF MS: *m*/*z*: 854 $[M+H]^+$.

4.1.4. P-OPV2. To a solution of porphyrin bisphosphonium salts (45 mg, 0.03 mmol) and OPV2 (20 mg, 0.09 mmol) in 25 mL of dry CH_2Cl_2 was added lithium ethoxide solution (0.25 mL, 1.0 M in ethanol) dropwise via a syringe for 2 h at room temperature. After concentration on a rotary evaporator, this solution was loaded onto a silica gel column and eluted with a mixture of petroleum ether and methylene chloride (1:1 v/v). This afforded the product as purple solid (6 mg, 18%). ^{1}H NMR ($CDCl_3$): δ (ppm) −2.59 (s, 2H), 1.84 (s, 12H), 2.65 (s, 6H), 7.18 (s, 2H), 7.25 (s, 2H), 7.28 (s, 6H), 7.39 (t, 4H, J=7.6 Hz), 7.45 (t, 3H, J=3.6 Hz), 7.55 (t, 6H, J=8.0 Hz), 7.60 (d, 3H, J=8.0 Hz), 7.67 (d, 3H, J=8.0 Hz), 7.90 (d, 3H, J=8.0 Hz), 8.09–8.13 (m, 3H), 8.21–8.25 (m, 3H), 8.67–8.70 (m, 2H), 8.76–8.78 (m, 2H), 8.82 (d, 1H, J=4.7 Hz), 8.82 (d, 1H, J=4.7 Hz), 8.85 (d, 1H, J=4.8 Hz), 8.91 (d, 1H, J=4.7 Hz), 8.94 (d, 1H, J=4.7 Hz). MALDI-TOF MS: *m*/*z*: 1106 $[M+H]^+$. Anal. Calcd for $C_{82}H_{66}N_4$: C, 88.93; H, 6.01; N, 5.06. Found: C, 88.78; H, 5.97; N, 5.12.

4.1.5. P-OPV4. Similar procedure to prepare P-OPV2 was carried out to afford P-OPV4 as purple solid. Yield: 7 mg (20%). ^{1}H NMR ($CDCl_3$): δ (ppm) −2.59 (s, 2H), 0.90 (t, 12H, J=6.0 Hz), 1.25–1.28 (m, 72H), 1.54–1.58 (m, 12H), 1.85–1.91 (m, 8H), 2.63–2.66 (m, 6H), 4.08–4.12 (m, 8H), 7.14–7.18 (m, 8H), 7.22–7.24 (m, 2H), 7.27–7.29 (m, 6H), 7.35–7.39 (m, 4H), 7.44–7.45 (m, 2H), 7.50–7.54 (m, 14H), 7.60–7.68 (m, 8H), 7.89 (d, 2H, J=7.6 Hz), 8.10 (d, 2H, J=7.6 Hz), 8.22 (d, 2H, J=7.9 Hz), 8.47–8.55 (m, 8H), 8.69–8.71 (m, 4H), 8.86–8.87 (m, 4H). MALDI-TOF MS: *m*/*z*: 2253 $[M+H]^+$. Anal. Calcd for $C_{162}H_{186}N_4O_4$: C, 86.35; H, 8.32; N, 2.49. Found: C, 86.27; H, 8.26; N, 2.40.

4.1.6. P-OPV2-Zn. To a solution of P-OPV2 (11 mg, 0.01 mmol) in 25 mL of THF solution was added $Zn(CH_3COO)_2 \cdot 2H_2O$ (43 mg, 0.13 mmol) and stirred for 2 h. This solution was loaded onto a silica gel column and eluted with methylene chloride. This gave the product as purple solid. ^1H NMR ($CDCl_3$): δ (ppm) 1.84 (s, 12H), 2.63 (s, 6H), 7.11–7.12 (m, 4H), 7.18 (s, 3H), 7.28 (s, 4H), 7.39 (t, 4H, J=7.6 Hz), 7.45 (d, 3H, J=4.5 Hz), 7.51–7.52 (m, 14H), 7.56 (t, 2H, J=8.0 Hz), 7.60 (d, 2H, J=8.0 Hz), 7.67 (d, 2H, J=8.0 Hz), 7.90 (d, 2H, J=7.2 Hz), 8.23 (d, 2H, J=7.2 Hz), 8.79 (d, 2H, J=4.5 Hz), 8.95 (d, 2H, J=4.5 Hz). MALDI-TOF MS: m/z: 1169 $[M+H]^+$. Anal. Calcd for $C_{82}H_{64}N_4Zn$: C, 84.12; H, 5.51; N, 4.79. Found: C, 83.92; H, 5.52; N, 4.86.

4.1.7. P-OPV4-Zn. Similar procedure to prepare P-OPV2-Zn was carried out to afford P-OPV4-Zn as purple solid. ^1H NMR ($CDCl_3$): δ (ppm) 0.79–0.82 (m, 12H), 1.18–1.21 (m, 72H), 1.77 (s, 12H), 1.80–1.82 (m, 8H), 2.56 (s, 6H), 3.99 (t, 8H, J=6.0 Hz), 7.05–7.09 (m, 8H), 7.17–7.18 (m, 8H), 7.21 (s, 4H), 7.27–7.32 (m, 4H), 7.37–7.40 (m, 4H), 7.44–7.47 (m, 14H), 7.52–7.54 (m, 4H), 7.60–7.62 (m, 4H), 7.81–7.83 (m, 4H), 8.16–8.18 (m, 4H), 8.72 (d, 4H, J=4.5 Hz), 8.89 (d, 4H, J=4.5 Hz). MALDI-TOF MS: m/z: 2315 $[M+H]^+$. Anal. Calcd for $C_{162}H_{184}N_4O_4Zn$: C, 83.99; H, 8.01; N, 2.42. Found: C, 83.86; H, 7.95; N, 2.35.

Acknowledgements

This work was supported by the National Natural Science Foundation of China (20531060, 10474101, 20418001, 20571078, and 20421101) and the Major State Basic Research Development Program (2006CB300402).

Supplementary data

Fluorescence emission decay of P-OPVn (n=2, 4) and P-OPVn-Zn (n=2, 4), fluorescence excitation spectra, CV of P-OPV2 and P-OPV4, and the synthesis route of porphyrin bisphosphonium salts. Supplementary data associated with this article can be found in the online version, at doi:10.1016/j.tet.2006.10.029.

References and notes

1. (a) Maruyama, K.; Osuka, A. *Pure Appl. Chem.* **1990**, *62*, 1511; (b) Gust, D.; Moore, T. A. *Science* **1989**, *244*, 35; (c) Gust, D.; Moore, T. A. *Top. Curr. Chem.* **1991**, *159*, 103; (d) Wasielewski, M. R. *Chem. Rev.* **1992**, *92*, 435; (e) Paddon-Row, M. N. *Acc. Chem. Res.* **1994**, *27*, 18; (f) Bard, A. J.; Fox, M. A. *Acc. Chem. Res.* **1995**, *28*, 141; (g) Piotrowiak, P. *Chem. Soc. Rev.* **1999**, *28*, 143; (h) Ward, M. W. *Chem. Soc. Rev.* **1997**, *26*, 365.
2. (a) Hayashi, T.; Ogoshi, H. *Chem. Soc. Rev.* **1997**, *26*, 355; (b) Feldheim, D. L.; Keating, C. D. *Chem. Soc. Rev.* **1998**, *27*, 1; (c) *Introduction of Molecular Electronics*; Petty, M. C., Bryce, M. R., Bloor, D., Eds.; Oxford University Press: New York, NY, 1995.
3. (a) Diesenhofer, J.; Michel, H. *Angew. Chem., Int. Ed. Engl.* **1989**, *28*, 829; (b) Feher, J. P.; Allen, M. Y.; Okamura, M. Y.; Rees, D. C. *Nature* **1989**, *339*, 111.
4. (a) Ferri, A.; Polzonetti, G.; Licoccia, S.; Paolesse, R.; Favretto, D.; Traldi, P.; Russo, M. V. *J. Chem. Soc., Dalton Trans.* **1998**, *23*, 4063; (b) George, S. J.; Ajayaghosh, A.; Jonkheijm, P.; Schenning, A. P. H. J.; Meijer, E. W. *Angew. Chem., Int. Ed.* **2004**, *43*, 3422; (c) Gaylord, B. S.; Wang, S.; Heeger, A. J.; Bazan, G. C. *J. Am. Chem. Soc.* **2001**, *123*, 6417; (d) Jonkheijm, P.; Hoeben, F. J. M.; Kleppinger, R.; van Herrikhuyzen, J.; Schenning, A. P. H. J.; Meijer, E. W. *J. Am. Chem. Soc.* **2003**, *125*, 15941; (e) Armaroli, N.; Accorsi, G.; Rio, Y.; Ceroni, P.; Vicinelli, V.; Nierengarten, J. F. *New J. Chem.* **2004**, *28*, 1627.
5. (a) Nagata, T.; Osuka, A.; Maruyama, K. *J. Am. Chem. Soc.* **1990**, *112*, 3054; (b) Wagner, R. W.; Lindsey, J. S. *J. Am. Chem. Soc.* **1994**, *116*, 9759; (c) Kumble, R.; Palese, S.; Lin, V. S. Y.; Therien, M. J.; Hochstrasser, R. M. *J. Am. Chem. Soc.* **1998**, *120*, 11489; (d) Cho, H. S.; Rhee, H.; Song, J. K.; Min, C. K.; Takase, M.; Aratani, N.; Cho, S.; Osuka, A.; Joo, T.; Kim, D. *J. Am. Chem. Soc.* **2003**, *125*, 5849; (e) Kim, D.; Osuka, A. *J. Phys. Chem. A* **2003**, *107*, 8791; (f) Choi, M. S.; Aida, T.; Yamazaki, T.; Yamazaki, I. *Angew. Chem., Int. Ed.* **2001**, *40*, 3194; (g) Takei, F.; Hayashi, H.; Onitsuka, K.; Kobayashi, N.; Takahashi, S. *Angew. Chem., Int. Ed.* **2001**, *40*, 4092; (h) Fujitsuka, M.; Okada, A.; Tojo, S.; Takei, F.; Onitsuka, K.; Takahashi, S.; Majima, T. *J. Phys. Chem. B* **2004**, *108*, 11935; (i) de Witte, P. A. J.; Castriciano, M.; Cornelissen, J. J. L. M.; Scolaro, L. M.; Nolte, R. J. M.; Rowan, A. E. *Chem.—Eur. J.* **2003**, *9*, 1775; (j) Jiang, B.; Yang, S.; Jones, W. E., Jr. *Chem. Mater.* **1997**, *9*, 2031; (k) Wolffs, M.; Hoeben, F. J. M.; Beckers, E. H. A.; Schenning, A. P. H. J.; Meijer, E. W. *J. Am. Chem. Soc.* **2005**, *127*, 13484.
6. (a) Xue, C.; Luo, F.-T. *J. Org. Chem.* **2003**, *68*, 4417; (b) Jørgensen, M.; Krebs, F. C. *J. Org. Chem.* **2004**, *69*, 6688; (c) Dudek, S. P.; Sikes, H. D.; Chidsey, C. E. D. *J. Am. Chem. Soc.* **2001**, *123*, 8033.
7. Jiang, B.; Jones, W. E., Jr. *Macromolecules* **1997**, *30*, 5575.
8. Laha, J. K.; Dhanalekshmi, S.; Taniguchi, M.; Ambroise, A.; Lindsey, J. S. *Org. Process Res. Dev.* **2003**, *7*, 799.
9. (a) Wagner, R. W.; Lindsey, J. S.; Seth, J.; Palaniappan, V.; Bocian, D. F. *J. Am. Chem. Soc.* **1996**, *118*, 3996; (b) Wagner, R. W.; Johnson, T. E.; Lindsey, J. S. *J. Am. Chem. Soc.* **1996**, *118*, 11166.
10. Ono, N.; Tomita, H.; Maruyama, K. *J. Chem. Soc., Perkin Trans. 1* **1992**, 2453.
11. (a) Virgili, T.; Lidzey, D. G.; Bradley, D. D. C. *Adv. Mater.* **2000**, *12*, 58; (b) Guo, T. F.; Chang, S. C.; Yang, Y.; Kwong, R. C.; Thompson, W. E. *Org. Electron.* **2000**, *1*, 15.
12. (a) Seybold, P. G.; Gouterman, M. *J. Mol. Spectrosc.* **1969**, *31*, 1; (b) Xiao, S. Q.; El-Khouly, M. E.; Li, Y. L.; Gan, Z. H.; Liu, H. B.; Jiang, L.; Araki, Y.; Ito, O.; Zhu, D. B. *J. Phys. Chem. B* **2005**, *109*, 3658; (c) Hascoat, P.; Yang, S. I.; Lammi, R. K.; Alley, J.; Bocian, D. F.; Lindsey, J. S.; Holten, D. *Inorg. Chem.* **1999**, *38*, 4849.
13. (a) van Hal, P. A.; Knol, J.; Langeveld-Voss, B. M. W.; Meskers, S. C. J.; Hummelen, J. C.; Janssen, R. A. J. *J. Phys. Chem. A* **2000**, *104*, 5974; (b) Langa, F.; Gomez-Escalonilla, M. J.; Rueff, J.-M.; Duarte, T. M. F.; Nierengarten, J. F.; Palermo, V.; Samor, P.; Rio, Y.; Accorsi, G.;

Armaroli, N. *Chem.—Eur. J.* **2005**, *11*, 4405; (c) Peeters, E.; van Hal, P. A.; Knol, J.; Brabec, C. J.; Sariciftci, N. S.; Hummelen, J. C.; Janssen, R. A. J. *J. Phys. Chem. B* **2000**, *104*, 10174.

14. Van Hutten, P. F.; Krasnikov, V. V.; Hadziioannou, G. *Acc. Chem. Res.* **1999**, *32*, 257.
15. Yang, S. I.; Seth, J.; Strachan, J. P.; Gentemann, S.; Kim, D.; Holten, D.; Lindsey, J. S.; Bocian, D. F. *J. Porphyrins Phthalocyanines* **1999**, *3*, 117.
16. (a) Zhang, Y. C.; Zhu, W. H.; Wang, W. J.; Tian, H.; Su, J. H.; Wang, W. C. *J. Mater. Chem.* **2002**, *12*, 1294; (b) Wang, B.; Wasielewski, M. R. *J. Am. Chem. Soc.* **1997**, *119*, 12.